Characterization of a Viroid-Derived RNA Promoter for the DNA-Dependent RNA Polymerase from *Escherichia coli*†

Martin Pelchat, Catherine Grenier, and Jean-Pierre Perreault*

RNA Group/Groupe ARN, Département de Biochimie, Faculté de Médecine, Université de Sherbrooke, Sherbrooke, Québec, J1H 5N4, Canada

Received January 25, 2002; Revised Manuscript Received March 11, 2002

ABSTRACT: This paper attributes a novel function, namely, that of transcriptional promoter, to the self-complementary, self-cleaving hammerhead RNA sequences found in RNA derived from the peach latent mosaic viroid (PLMVd). The features of this RNA promoter, which adopts a hairpin structure that can be utilized by *Escherichia coli* RNA polymerase (RNAP) for in vitro transcription, that trigger the RNAP driven transcription and are responsible for the specific initiation of synthesis are described. The essential requirement for initiation is a basepaired uridine adjacent to the loop. The presence of a loop composed of at least six nucleotides connected to a relatively unstable stem significantly increases the level of initiation. Finally, we present several insights into the mechanism of the RNAP which reveal that it behaves differently with an RNA template as compared to a DNA one.

Several DNA-dependent RNA polymerases (RNAP)[1] have been shown to use RNA as template when a suitable one is offered. For example, T7 RNAP has been reported to replicate an RNA contaminant of unknown genetic origin, in a commercial batch of the enzyme (*1*). It has also been shown that high concentrations of T7 RNAP are able to replicate a large variety of different RNA species when incubated for extended time periods (*2*). This T7 RNAP based RNA amplification mechanism was proposed to be analogous to what is observed with viral RNA-dependent RNAPs; that is only single-stranded templates are accepted, and both, the template and its complementary replica are released as single strands (*2*). Another DNA-dependent RNAP frequently reported to support transcription in the presence of an RNA template is that from *Escherichia coli* (*E. coli*). This RNAP has been shown to nonspecifically replicate viroids in vitro, although it should be noted that these experiments were performed in the presence of manganese which significantly reduces polymerase specificity (*3*). Additionally, this RNAP is capable of amplifying selected small, random, RNA polymers (*4*, *5*).

From the natural RNAs that make use of the potential of DNA-dependent RNAP to replicate themselves, viroids are the simplest and the best characterized. They are small (∼300 nucleotides, nt), single-stranded, circular RNAs that infect higher plants causing significant losses in the agricultural industry (reviewed in ref *6*). They neither encode protein, nor are they encapsidated. As a consequence, viroids are RNA genomes possessing both genotypic and phenotypic properties. They replicate via a rolling circle mechanism involving exclusively RNA intermediates, and are therefore ideally suited for analyses of RNA amplification by DNA-dependent RNAP. Viroids are classified into two separate groups. Most viroids fall into the pospiviroidae group, whose members fold into a rodlike secondary structure that includes a highly conserved central region and have been shown to accumulate in the nucleus (*6*−*9*). A role for nuclear RNAP II in the replication of pospiviroidae is suggested by the observations that it is inhibited by low concentrations of α-amanitin (*7*), and that, in vivo, citrus exocortis viroid was found to be associated with the largest subunit of RNAP II in tomato (*10*). A similar sensitivity to α-amanitin was also reported using an in vitro transcription extract prepared from a noninfected potato cell culture exhibiting transcriptional activity on added circular potato spindle tuber viroid (PSTVd) RNA as template (*11*).

The remaining three viroids form the avsunviroidae group. Avocado sunblotch viroid (ASBVd) is believed to adopt a rodlike secondary structure, while both peach latent mosaic viroid (PLMVd; Figure 1) and chrysanthemum chlorotic mottle viroid are believed to have complex branched structures (*12*−*15*). These RNA species lack a conserved central region, but exhibit self-cleavage of their RNA multimers using hammerhead motifs (*6*, *12*). Their polymerization step is clearly different from that of the pospiviroidae as it is unaffected by high levels of α-amanitin, and they are observed to accumulate in the chloroplast (*16*, *17*). Two main chloroplastic RNAPs have been described: the plastid-encoded polymerase, which possesses a multisubunit structure similar to that of the *E. coli* enzyme, and a single-unit nuclear-encoded polymerase that resembles phage RNAP (reviewed in ref *18*). On the basis of the fact that a protein extract from avocado chloroplast replicating ASBVd was

† This work was supported by a grant from the Natural Sciences and Engineering Research Council (NSERC) of Canada to J.P.P. The RNA group is supported by grants from both the Canadian Institutes of Health Research (CIHR) and Fonds FCAR (Québec). M.P. is the recipient of a postdoctoral fellowship from the CIHR. J.P.P. is an Investigator of the CIHR.

* Corresponding author: Phone: (819) 564-5310. Fax: (819) 564-5340. E-mail: jperre01@courrier.usherb.ca.

[1] Abbreviations: PLMVd, peach latent mosaic viroid; ASBVd, avocado sunblotch viroid; PSTVd, potato spindle tuber viroid; *E. coli*, *Escherichia coli*; RNAP, RNA polymerase; K_D, dissociation constant.

10.1021/bi025595k CCC: $22.00
Published on Web 04/27/2002

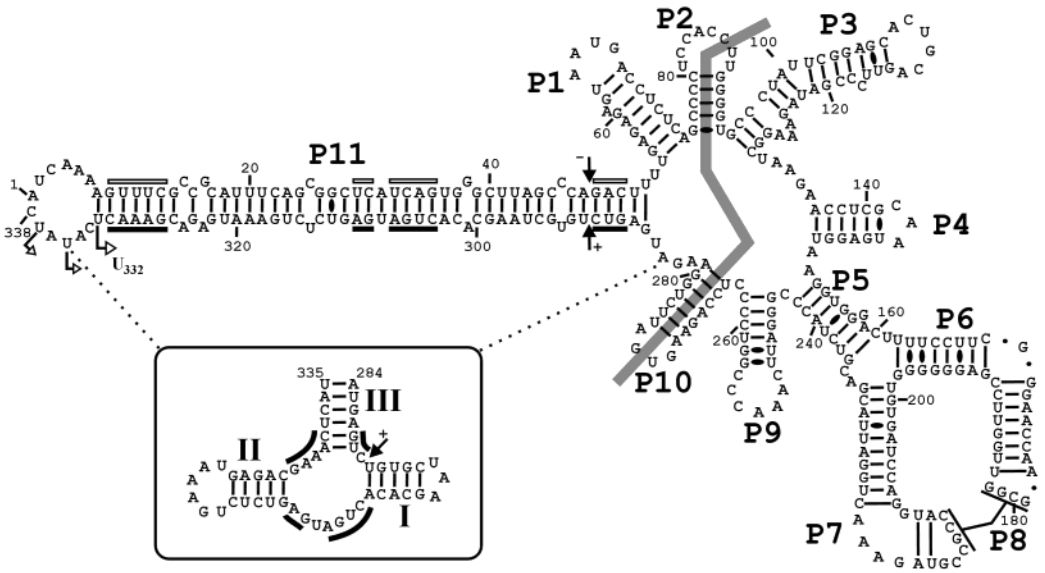

FIGURE 1: PLMVd sequence and proposed secondary structure. The helix numbering is in accordance with Bussière et al. (*16*). The hammerhead consensus sequences are indicated by open bars for minus polarity and by closed bars for plus polarity, and the cleavage sites by arrows. The large gray line separates the right domain from the left one, which was previously shown to initiate replication at the positions indicated by the white arrows (see left-terminal loop; *20*). The inset shows the sequence and secondary structure of the plus polarity hammerhead motif with its stems numbered.

resistant to tagetitoxin, the phage-like RNAP has been proposed to support the replication of this viroid (*19*). In contrast, the bacterial-like RNAP from peach chloroplasts was suggested as the enzyme supporting PLMVd replication in peach leaves (*20*). More specifically, *E. coli* DNA-dependent RNAP was shown to specifically initiate the replication of PLMVd in vitro using derived-transcripts as template (see below). It is doubtful that these two related viroids with similar replication strategies would have evolved in such a manner that they are transcribed by different enzymes in chloroplasts. However, these results do not exclude the possibility that ASBVd and PLMVd use different RNAPs for their respective replications, particularly since it is known that these viroids share some features, but differ in others.

In the case of PLMVd, initial results of an in vitro transcription assay using *E. coli* RNAP and various PLMVd-derived transcripts has been reported (*20*). In this enzymatic assay, magnesium was the only bivalent cation present, thereby preserving the specificity of the RNAP. The *E. coli* RNAP cannot be substituted for by wheat germ RNAP II, T7 or SP6 phage RNAP, indicating that the transcription is enzyme specific. The *E. coli* RNAP initiation sites correspond to the 5′-ends of two small (280 nt) PLMVd-related RNAs found in infected peach leaves. In contrast to what was observed in the case of the replication of ASBVd (*19*), tagetitoxin has only a weak effect on the in vitro transcription from PLMVd RNA templates by *E. coli* RNAP, suggesting that the polymerase behaves differently when using RNA instead of DNA as template. Regardless of the polarity of the PLMVd strand used as template, the primary initiation site was fixed at the first uridine adjacent to the left-terminal loop, specifically at positions U_{332} and U_7, in the plus and minus polarity strands, respectively (Figure 1). Secondary sites were also observed at specific pyrimidine residues found within this loop. Using various PLMVd-derived transcripts as templates, it was proposed that the domain formed by stems P10 to P2, which includes the self-complementary hammerhead sequences, was both essential and sufficient for the initiation of transcription to occur (i.e., the domain formed by stems P3 to P9 can be deleted without loss of transcriptional activity, Figure 1).

The goal of this work was to (i) characterize this transcription assay and (ii) provide the first description of the features of an RNA promoter that trigger the *E. coli* RNAP driven transcription and that allow the specific initiation of its in vitro reaction. In the course of this work, several insights into the mechanism of a DNA-dependent RNAP acting on an RNA template were revealed and are described here. Although nonphysiological, this in vitro system corresponds to the first characterization of a viroid promoter.

MATERIALS AND METHODS

Synthesis of PLMVd-Derived RNAs. The 94-nt RNA template of minus polarity was produced from plasmid pPD1, digested with *Mbo*II, as described previously (*21*). The 161-nt transcript of plus polarity was synthesized from a DNA template generated by PCR, using Vent DNA Polymerase (New England Biolabs), from plasmid pPD1 using sense (5′-GGAATTCTAATACGACTCACTATAGG_{273}GATTCTGGAAGATGAGGGT GTGCTAAGCAC$_{302}$-3′) and antisense (5′-GGAATTC$_{86}$GGTGGAGGGGCTGAG$_{72}$-3′; the underlined nucleotides indicate T7 promoter and *Eco*RI restriction site) oligonucleotide primer. The small P11-derived RNA templates were synthesized using double-stranded DNA oligonucleotides possessing a T7 RNA promoter. After in vitro runoff transcription using T7 RNA polymerase, DNase (RNase-free) treatment, and nucleic acid precipitation, the transcripts were fractionated through denaturing 5 or 10% polyacrylamide gels (PAGE) in 1× TBE (100 mM Tris-borate, pH 8.3, 1 mM EDTA) containing 7 M urea buffer. The RNA templates were detected by UV shadowing, excised, eluted in 500 mM ammonium acetate/0.1% sodium dodecyl sulfate (SDS) solution, precipitated,

resuspended in 1 mM EDTA pH 8.0, purified by passage through Shephadex G-50 spun columns (Amersham Pharmacia Biotech) and conserved at −70 °C.

Transcription Assays using E. coli RNAP. Transcription reactions were performed according to the manufacturer's recommended protocol (Amersham Pharmacia Biotech). Briefly, RNA templates (50 pmol) were resuspended in 50 μL of transcription buffer (40 mM Tris-HCl, pH 8.0/10 mM $MgCl_2$/150 mM KCl/5 mM dithiothreitol (DTT)/5 μg/mL BSA) containing 0.2 mM NTP and 50 μCi of either [α-^{32}P]-GTP or [γ-^{32}P]ATP (3000 Ci/mmol) for the radioactive reactions (Amersham Pharmacia Biotech). *E. coli* RNAP (0.9 pmol; Amersham Pharmacia Biotech) was then added and the reactions incubated at 37 °C for 60 min. In some cases, either *E. coli* holo- or core-RNAP (0.9 pmol each; Epicentre Technologies) was used in either the presence or the absence of 5 pmol of purified his-tagged σ^{70} (see below). The reactions were stopped by adding 25 μL of stop buffer (80% formamide/10 mM EDTA, pH 8.0/0.1% each of xylene cyanol (XC) and bromophenol blue (BPB)), and were then fractionated through either 12 or 20% PAGE gels as described above. The intensity of each individual band (from three independent experiments), was determined by phosphorimager scanning, and the relative amounts of RNA quantified using the ImageQuant software (Molecular Dynamics) so as to be able to compare to the amount of products formed with that of the 161-nt RNA of plus polarity.

Primer Extension of RNA Products. The RNA was heated for 5 min at 65 °C with 1 pmol of ^{32}P-5′-end-labeled oligonucleotide in 5 μL of annealing buffer (50 mM Tris-HCl, pH 8.3/10 mM $MgCl_2$/80 mM KCl solution), and the mixture was then snap frozen by immersion in a −80 °C ethanol/dry ice for 2 min. Synthesis was initiated by adding 4 units of avian myeloblastosis virus reverse transcriptase (Amersham Pharmacia Biotech) in 5 μL of ice cold annealing buffer containing 8 mM DTT and 4 mM dNTP, and allowed to proceed at 42 °C for 30 min. The reaction products were then fractionated by 10% PAGE, and revealed by phosphorimaging.

*Overproduction and Purification of His-Tagged σ^{70}. rpo*D mutants made using pQE30-rpoD (*22*, *23*) were transformed into *E. coli* strain BL21(DE3)pLysS, and his-tagged proteins were purified as described by Wilson and Dombroski (*23*). Briefly, protein expression was induced by the addition of isopropyl-β-D-thiogalactopyranoside (IPTG) to 2 mM final concentration to exponentially growing cultures. After 3−4 h of growth at 37 °C, the cells were harvested by centrifugation, resuspended in binding buffer (5 mM imidazole/0.5 M NaCl/20 mM Tris-HCl, pH 7.9) and lysed by sonication. The resulting lysate was centrifuged, and the σ^{70}-containing pellet resuspended in binding buffer containing 6 M urea. The his-tagged σ^{70} was then purified using a Ni^{2+}-activated resin (Qiagen), and eluted with the same buffer containing increasing concentrations of imidazole as described by the manufacturer. Purified, denatured extracts were dialyzed overnight at 4 °C against 50 mM Tris-HCl, pH 7.9/1 mM EDTA/0.1 mM DTT/50 mM NaCl/50% glycerol solution. The protein concentration and purity were estimated by Coomassie blue staining of SDS−PAGE gels. Samples found to be more than 95% pure were conserved at −80 °C.

Electrophoretic Mobility-Shift Assay. Double-stranded σ^{70}-driven DNA promoter (5′GCTAACTTGTTTTGACACCGGGTCTATTTGGTGGTATAATAGATTCATACATTTTTGCCT-3′; the underlined nucleotides indicate, in order, the −35 and −10 boxes and the initiation site), total tRNA from *E. coli* (Roche Diagnostic) and P11.60 RNA fragment were end-labeled with [γ-^{32}P]ATP using T4 polynucleotide kinase according to the manufacturer's recommended protocol (New England Biolabs). The σ^{70}-driven DNA promoter was derived from the −50 to +10 sequence of the *Bacillus subtilis glt*X promoter (*24*) in which the −10 and −35 boxes were altered to the *E. coli* consensus sequences (*25*). Radiolabeled template (1 pmol) was dissolved in a final volume of 10 μL of transcription buffer containing increasing amounts of either *E. coli* holo- (Pharmacia or Epicentre Technologies) or core-RNAP (Epicentre Technologies). After incubating at room temperature for 60 min, 3 μL of 30% glycerol/0.25% XC, and 0.25% BPB solution were added, and the resulting solution electrophoresed through a native 5% PAGE gel (bis:acrylamide, 49:1) at room temperature in 1× TBE buffer at low voltage. The gels were then exposed to a phosphor screen, and the bands were quantified as above. Competition EMSA assays were performed as described above, with the exception that the amount of enzyme was kept constant at 0.9 pmol, and 20 pmol of either the DNA promoter or total tRNA from *E. coli* were added.

RESULTS

Several initial experiments, using both different conditions and various templates, were performed to characterize the transcription assay. For all templates discussed in this article, the assays were performed in the presence of either one added nucleotide (i.e., GTP), or of all four nucleotides (NTPs), to differentiate between template extension (i.e., 3′-end addition) and synthesis of new RNA molecules (i.e., transcription), respectively. A typical gel using a 60-nt RNA template derived from the P11 domain is shown in Figure 2. In the presence of [α-^{32}P]GTP, template extension was detected primarily in the upper portion of the gel. Under transcription conditions (i.e., with the four NTPs present), additional short specific products that correspond to initiations occurring at the first uridine of the adjacent stem (U_{332}), and on the uridine residues in the left-terminal loop (U_{335} and U_{337}), were detected (Figure 2B). These initiation sites were identified by primer extension (data not shown), and correspond to those reported previously with longer PLMVd-derived templates (*20*). Moreover, the apparent sizes of the generated RNA products are consistent with those of transcripts whose 5′-ends correspond to the reported start site of transcription. Since newly in vitro transcribed RNAs contain a 5′-terminal triphosphate group (pppN), the assays were performed in the presence of [γ-^{32}P]ATP. This simplifies the analysis because any templates that are only extended are not labeled (i.e., not radioactive). These reactions gave the same transcription products as those performed in the presence of [α-^{32}P]GTP (Figure 2B). It should be noted that since there is less radioactivity per product, the intensities of the bands obtained in transcription experiments using [γ-^{32}P]ATP are weak. This experiment confirms that we are observing the initiation of synthesis of new RNA strands. The amount of products formed in the presence of [γ-^{32}P]ATP was compared that to formed when using [α-^{32}P]GTP, after normalization of the latter for the number of guanosine residues in the products.

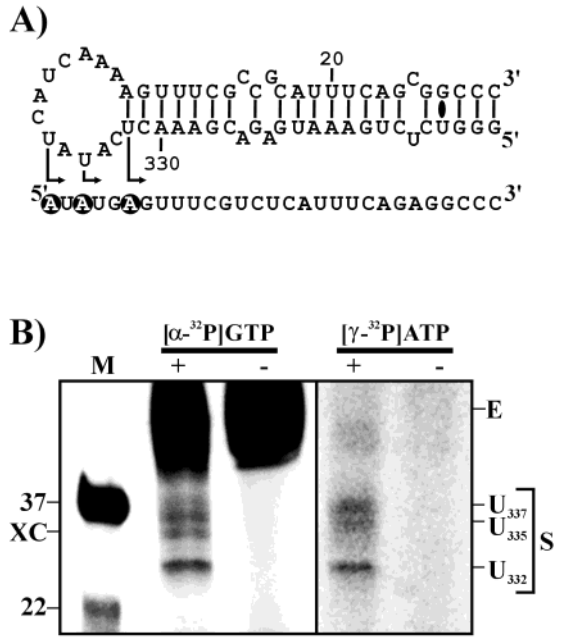

FIGURE 2: P11.60 RNA template and typical autoradiograms of transcription assays. (A) Sequence and secondary structure of the P11.60 RNA template used. Initiation sites are shown by black circles, and RNA product are shown. (B) The assays were performed in the presence of either only GTP (−) or of all four nucleotides (+), and in the presence of either [α-^{32}P]GTP or [γ-^{32}P]-ATP as the radiolabeled nucleotide. The transcription products (S) are indicated by the nucleotide from which the transcripts originate on the template. Extension products (E), xylene cyanol (XC), and the positions of RNA size markers are indicated adjacent to the gel. Due to the low intensity of the bands obtained in transcription reactions using [γ-^{32}P]ATP, those lanes have been overexposed.

In each case, we found similar amounts of products, indicating that the two transcription protocols were analogous, and that adenosine triphosphate was the 5′-end nucleotide in every instance.

As previously described using complete PLMVd RNA as template (*20*), several experiments were performed to characterize this enzymatic assay (data not shown). For example, the absence of DNA contaminants was confirmed by adding DNase either prior to or after transcription. The product bands did not originate from the degradation of the template used as they were not detected when the incubation was performed using radiolabeled RNA templates in the presence of nonradioactive NTPs. However, they were detected when transcription was performed in the presence of nonradioactive NTP and the resulting RNA molecules 3′-end-labeled using T4 RNA ligase and [α-^{32}P]pCp. They were also detected when transcription was carried out using [γ-^{32}P]-ATP as the labeled nucleotide, showing that the RNAs produced contain a 5′-terminal triphosphate group and indicating the de novo initiation of transcription. Taken together, these results unambiguously prove that what we were observing was indeed specific transcription from our RNA templates catalyzed by the *E. coli* RNAP, and not species generated by either template extension or the specific hydrolysis of the templates.

Defining the PLMVd Promoter Domain. To define the minimal sequence and structure capable of acting as an RNA promoter, PLMVd-derived templates were synthesized by in vitro transcription from a DNA cloned insert (94-nt), a PCR-amplified product (161-nt), or from double-stranded oligonucleotides harboring a T7 promoter for the production of RNA in large amounts (see Figures 3 and 4 for all templates). The resulting RNA molecules were gel-purified and tested as templates in the *E. coli* RNAP transcription assay. The nomenclature of the templates is as follows: (i) since all RNA templates are derived from the P11 stem, the three first characters (i.e., P11) were assigned to all of them; (ii) this is followed by their nucleotide length; and (iii) when required, their modification was compared to the wild-type P11 sequence. For example, P11.75 stands for a P11-derived template composed of 75 nt, while P11.75GC represents a P11.75 RNA having a greater number of GC base pairs within the basepaired region (Figure 3).

For each RNA template, the amount of product formed, based on at least three independent experiments, was estimated by combining the amount of all bands corresponding to new strands (using a phosphorimager) to evaluate its efficiency as a template for transcription. This allowed us to compare the amount of product formed to that obtained using the plus polarity 161-nt RNA template. This latter template was used as a basis of comparison in both this study and in the previous one that includes the results using full-length PLMVd strands as templates (*20*).

The results of the templates used for the identification of the minimal sequence and structure required to be able to act as an RNA promoter are summarized in Figure 3. Templates P11.75 and P11.60, which possess 28 and 21 basepairs (bp) stems, respectively, gave slightly higher levels of transcription than did the 161-nt template. Similar observations have been reported when comparing the transcription efficiencies of longer PLMVd-derived templates, more specifically the observation that smaller templates such as the 161-nt one gave greater amounts of products than did full-length PLMVd (*20*). Long RNA strands can adopt alternative secondary structures, such as the hammerhead ones, which might impede transcription. The gain in transcription efficiency observed with smaller RNA templates is more likely due to the presence of a more homogeneous promoter structure in these templates. Finally, the P11.26 template, which possesses a short 7-bp stem, still produced a detectable, through reduced, level of transcription, suggesting that more energetically stable stems, such as those predicted for both the P11.60 and P11.75 templates, may produce higher levels of transcription (Figure 3). It is noteworthy that the initiation sites were identical for all of these templates. Thus, the P11 domain can be reduced by about half without significantly affecting the transcription, and both the P11.60 and P11.75 molecules appear to be ideal templates for continuing the analysis.

To confirm that the PLMVd-derived strands of both polarities can be considered as identical in terms of being an in vitro transcriptional promoter, an RNA molecule of 94-nt derived from the P11 domain of minus polarity was synthesized and tested (Figure 3). This template exhibited a transcription level similar to that of the 161-nt RNA of plus polarity, indicating that all of the elements required for the initiation of the synthesis of new strands of both PLMVd polarities in vitro by *E. coli* RNAP are located exclusively within the P11 domain. Although this in vitro transcription system is biologically unnatural, this result is in agreement with the observation that PLMVd intermediates of both polarities accumulate at similar levels in infected cells (*16*).

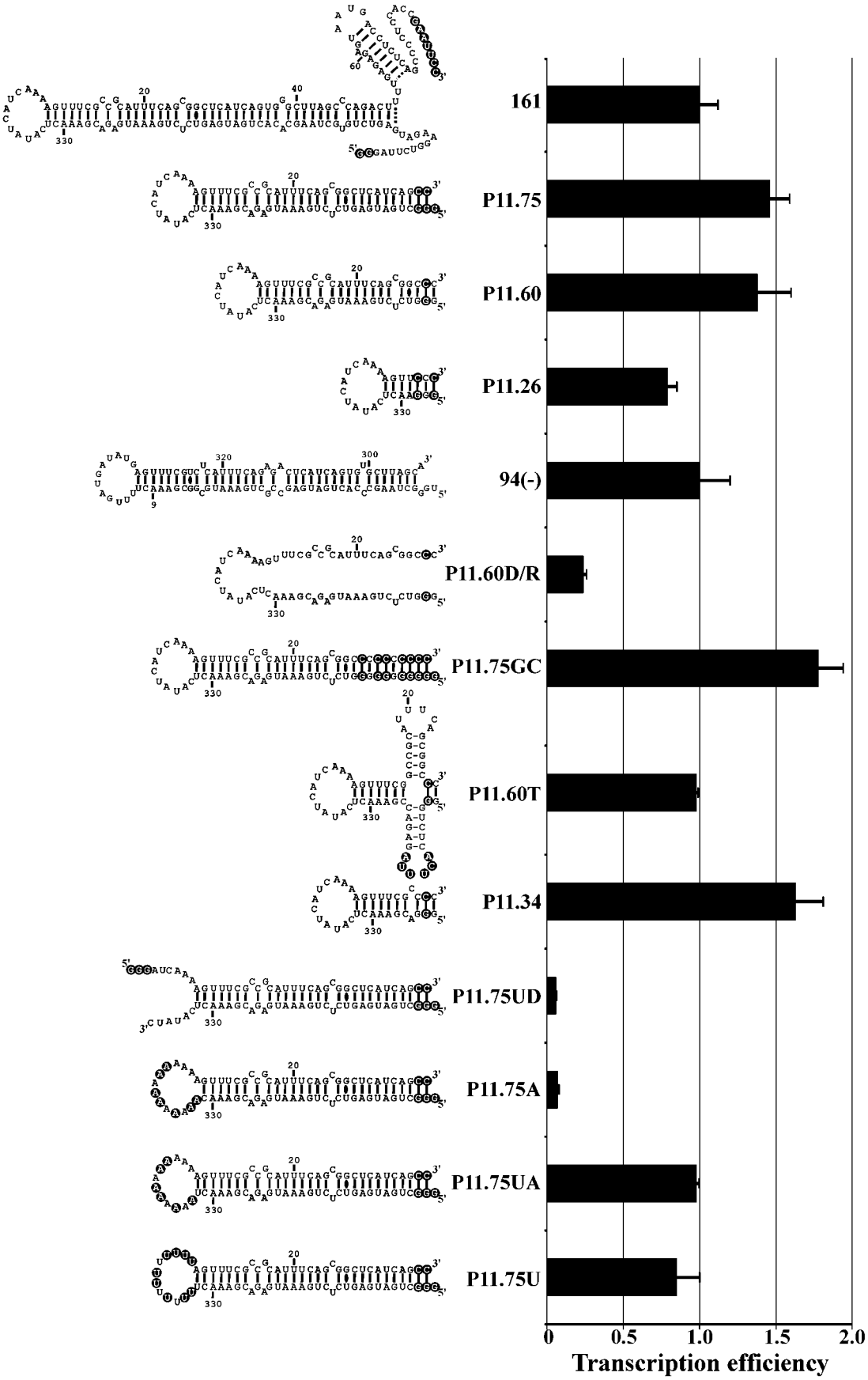

FIGURE 3: Influence of the stem length and structure on transcription efficiency. Various small PLMVd-derived RNAs were subjected to transcription assays and the resulting level of transcription quantified. The amount of product obtained from the 161-nt template was arbitrarily fixed to 1. The transcription efficiencies were calculated from three independent experiments, using the amounts of products formed in the presence of [γ-^{32}P]ATP or [α-^{32}P]GTP after normalization of the latter for the number of guanosine residues in the products. The nucleotides from the derived templates that differ from those of the original sequence (Figure 1) are circled.

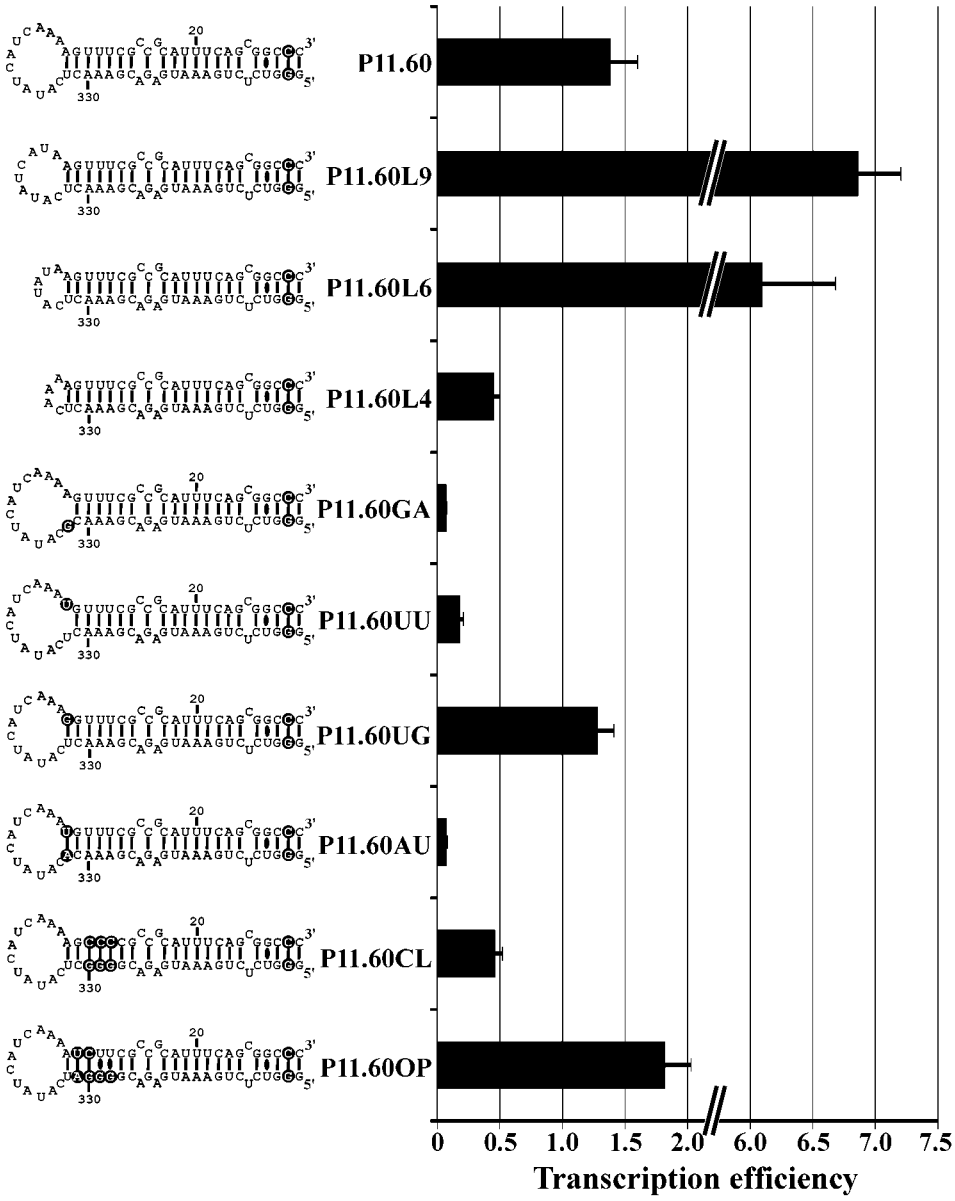

FIGURE 4: Influence of the loop composition, the initiation site, and the stem composition on transcription efficiency. Various small PLMVd-derived RNAs were subjected to transcription assays and the resulting levels of transcription quantified. The amount of product obtained from the 161-nt template was arbitrarily fixed to 1 (see Figure 3). The transcription efficiencies were calculated from three independent experiments, using the amounts of products formed in the presence of [γ-^{32}P]ATP or [α-^{32}P]GTP after normalization of the latter for the number of guanosine residues in the products. The nucleotides from the derived templates that differ from those of the original sequence (Figure 1) are circled.

PLMVd strands of both polarities share similar sequences and structures for the P11 domain, and most likely have similar promoter features in our system (i.e., compare the 161- and 94-nt RNA species).

The Rodlike Structure. Several experiments were performed with P11.60 and derived RNA templates to determine the importance of the rodlike conformation for the initiation of the transcription. For example, P11.60 was heat-denatured (1 min at 90 °C) and snap-cooled on ice (2 min) prior to the transcription assay, thereby favoring the adoption of alternative structures of higher free energy. In this case, the amounts of products detected were drastically reduced (P11.60D/R, Figure 3). All of the treatments tested indicate that the template must adopt the double-stranded structure (i.e., rodlike) for the most efficient transcription to be observed (data not shown). To gain support for this conclusion a template with a greater number of GC base pairs was synthesized (P11.75GC) (Figure 3). This template exhibited 20% more transcription than did the original P11.75, suggesting a correlation between transcription efficiency and stem stability. One of the putative alternative structures that the P11 domain may adopt is a cloverleaf-like conformation that includes the hammerhead stem II of both polarities (*14*). A template favoring this alternative conformation was designed by mutating six bases of P11.60 (P11.60T, Figure 3). This template exhibited a significant reduction in the level of transcription, supporting the idea that the rodlike structure is preferable. The transcription efficiency of P11.60T was only slightly higher than that of the small P11.26 template which also possesses a 7-bp long stem adjacent to the terminal loop. This small elevation in transcription is most likely caused by the higher thermodynamic stability of

P11.60T. To determine if it is possible to rescue the efficiency of transcription with a small template by inhibiting the formation of the cloverleaf structure, P11.34 was tested (Figure 3). This template, which has a 10-bp stem and could not adopt the cloverleaf conformation, had a transcription efficiency higher than those of both of the longer P11.75 and P11.60 templates. This result supports the idea that a proportion of the longer templates adopts alternative structures that reduce the level of transcription.

To verify whether the left-terminal loop was required, a P11.75-like template composed of two RNA strands folded together by heat denaturation and slow renaturation was tested (P11.75UD, Figure 3). This RNA is similar to P11.75, with the exception that it possesses an open region and three guanosine residues at the 5′-end of the upper strand for RNA production. No transcription was detected from this template (>25-fold lower as compared to P11.75). Thus, the loop appears to be essential for the initiation of the transcription. Previously, it was shown that the initiation occurs at position U_{332}, U_{335}, and U_{337} in the left-terminal loop. A template having the first nucleotides of the stem and the loop composed exclusively of adenosines did not support transcription (P11.75A, Figure 3), indicating the requirement for uridine residues in the template to have an adenosine as the initiating nucleotide as is the case when *E. coli* RNAP initiates from DNA templates (*26*). Transcription was rescued by either reverting the first base pair of the stem to A_7-U_{332} (P11.75UA), or by changing all of those nucleotides to uridine residues (P11.75U, Figure 3). No variation of the initiation sites was observed for P11.75U, while only initiation at U_{332} was detected for P11.75UA. Thus, specific sequences in the loop are not required, provided that there is an uridine for the initiation of transcription, specifically U_{332}. Clearly, these results reveal that the rodlike structure, including the terminal loop, the stem and U_{332}, constitute the promoter in vitro for *E. coli* RNAP.

Refinement of the Promoter Requirements. We used a deletion approach to determine the influence of the size of the left-terminal loop on transcription, using P11.60 as the initial template. As shown in Figure 4, templates P11.60L9, P11.60L6, and P11.60L4 possess loops of 9-, 6-, and 4-nt, respectively. The transcription efficiencies of P11.60L9 and P11.60L6 were 4−5-fold higher than that of the original P11.60 with its 12 nt loop, while that of P11.60L4 was 3-fold less. This reduction may be indicative of the need for a longer single-stranded RNA region for the binding of the enzyme to the template.

To determine the influence of the nucleotides in the neighborhood of the primary initiation site (U_{332}) on transcription, we initially studied the effect of mutations at this position. As observed with P11.75A, which includes an A at position 332, P11.60GA, which possesses a G at position 332 of P11.60, showed no transcription (Figure 4). These two mutants also eliminate the first base pair of the stem. To verify whether this base pair is important, templates P11.60UU, P11.60AU, and P11.60UG were synthesized (Figure 4). P11.60UU, which possesses a single-stranded U_{332}, showed a 6-fold lower level of transcription than did P11.60, suggesting that it is preferable to have this residue basepaired. In agreement, P11.60UG, which has the U_{332} basepaired with G_7 (rather than the $U_{332}A_7$ base pair present in P11.60), gave a level of transcription similar to that of the P11.60. In contrast, P11.60AU, in which the first base pair is inverted (i.e., $A_{332}U_7$), showed a significantly decreased transcription level and clearly illustrates the importance of having an uridine at position 332. We also noted that the initiation sites located in the loop were lost with both the P11.60AU and P11.60UU templates, indicating that U_{332} must be basepaired to observe initiation from within the loop.

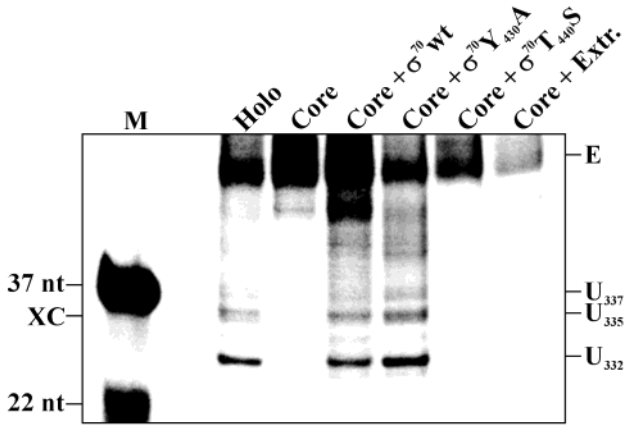

FIGURE 5: Transcription assays of a PLMVd-derived RNA template using various σ^{70} mutants. Transcription from P11.60 in the presence of either holo- or core-RNAP supplemented with either wild-type or mutated his-tagged σ^{70}. The transcription products are identified by the nucleotides from which the transcription was initiated. Extension products (E), xylene cyanol (XC), and the positions of RNA size markers are indicated adjacent to the gel.

For initiation to take place, the RNAP must also melt the double-stranded region that includes U_{332}. This stem has a relatively low GC base pair content (i.e., 4 AU/UA and 3 GC/CG bp), which may facilitate the melting step. We tested this hypothesis using a template with a higher GC content (P11.60CL, Figure 4), and observed a 3-fold decrease in transcription as compared to P11.60. In contrast, the P11.60OP template, which harbors GU wobble base pairs that provide the same GC content as P11.60, gave an increased level of transcription as compared to P11.60. This increase may be accounted for by the locally higher free energy of the stem (+0.9 kcal/mol at 37 °C when compare to P11.60, as calculated using the mfold program) (*27*). Thus, it appears that the relatively low GC content of the stem favors its melting by the RNAP.

Requirement for the σ^{70} Subunit. Initiation from a DNA promoter by *E. coli* RNAP has been extensively studied (reviewed in ref *22*); however, nothing is known about the enzyme requirements when using an RNA template. It is well-established that the σ^{70} subunit of *E. coli* RNAP binds to specific sequences on the DNA promoter located at positions −35 and −10 from the initiation site and acts as a specificity factor directing the binding of the enzyme near the initiation site (*26*). To verify whether the σ^{70} subunit is involved in a similar process when using PLMVd-derived RNA templates, in vitro transcription assays were performed using P11.60 RNA with either the holo- or core-RNAP (i.e., with or without σ^{70}, respectively; Figure 5). Regardless of whether σ^{70} was present, extension products were detected, indicating that this reaction is independent of this subunit. In contrast, the synthesis of new RNA strands was only observed in the presence of σ^{70}, showing an absolute requirement for this subunit for transcription to occur.

In contrast to known σ^{70}-driven DNA promoters, there is no region similar to the −35 and −10 boxes in the PLMVd-derived RNA promoters. We then investigated the roles of the σ^{70} subunit in the opening of the initiation fork, and whether its binding to the core-RNAP serves an essential function. Transcription assays using P11.60 as template were performed with either wild-type RNAP, or a reconstituted enzyme with purified his-tagged wild-type or mutant σ^{70} subunits (Figure 5). Transcription occurred in the presence of the core-enzyme supplemented with wild-type σ^{70} subunit. When the core-enzyme was complemented with a σ^{70} mutant deficient in fork opening (i.e., $Y_{430}A$), transcription occurred as efficiently as with wild-type σ^{70} at both 37 and 25 °C (data not shown). This contrasts to what is observed in the transcription from DNA templates where this mutant shows a significantly reduced level of transcription at 25 °C (data not shown; see also ref *28*). The observed lack of inhibition of transcription in the presence of the $Y_{430}A$ mutant may reflect the low stem stability of the RNA template used. However, when the transcription was performed in the presence of an RNA template containing mutations that stabilize the stem at the initation site (i.e., P11.60CL; Figure 4), similar transcription levels were obtained in the presence of either the $Y_{430}A$ mutant or the wild-type σ^{70} subunit (data not shown). Finally, no transcription was detected when the core-enzyme was complemented with the σ^{70}-$T_{440}S$ mutant, which exhibits unstable binding with the core-RNAP (*22*).

RNAP Promoter Affinity. The efficiency of a promoter frequently depends on how strongly it interacts with the polymerase. The binding affinity of the RNAP for a PLMVd-derived RNA was determined by electrophoretic mobility-shift assay. Labeled P11.60, total *E. coli* tRNA, or a strong σ^{70}-driven DNA promoter (1 pmol each) were allowed to bind with increasing amounts of *E. coli* RNAP for 60 min at room temperature, and then were subjected to electrophoresis through a nondenaturing 5% polyacrylamide gel. A typical gel, using P11.60 RNA as template with increasing amounts of *E. coli* holo-RNAP, is shown in Figure 6A. The σ^{70}-driven DNA promoter was found to strongly bind the holoenzyme, exhibiting a dissociation constant (K_D) of 20 ± 4 nM. This is an order of magnitude stronger than that observed for RNAP binding to the P11.60 template (K_D = 207 ± 17 nM), which is in turn only slightly stronger than the binding of an *E. coli* total tRNA mixture (K_D = 295 ± 39 nM). Finally, the binding affinity of P11.60 to the core-RNAP (i.e., without σ^{70}) was found to be almost equivalent (K_D = 199 ± 24 nM) to that for the holoenzyme, supporting the notion that σ^{70} does not participate in strand binding.

As a high K_D is often associated with a low binding specificity, enzyme binding to the P11.60 template was then studied by competition with either the *E. coli* total tRNA mixture, or with the σ^{70}-driven DNA promoter. Radiolabeled P11.60 (1 pmol) was incubated with no nucleic acid, total *E. coli* tRNA, or the σ^{70}-driven promoter (20 pmol each), and then the holoenzyme, the core-enzyme or purified his-tagged σ^{70} subunits were added (Figure 6B). The DNA promoter competed efficiently with P11.60 for both the holo- and core-RNAP, but not for the his-tagged σ^{70} subunit. We noted that the competition of the DNA promoter was higher for the holo- than for the core-enzyme. The fact that the DNA promoter competed with P11.60 for the RNAP suggests that the RNA and DNA templates bind to the same site on the enzyme. The total tRNA mixture competed less efficiently with the P11.60 template for both the holo- and core-enzyme, suggesting that although the binding of the RNAP to the PLMVd-derived RNA templates is weak, it is specific enough to not be easily displaced by a nonspecific competitor. In contrast, P11.60 binding to the his-tagged σ^{70} subunit can easily be inhibited by the tRNA mixture, but not by the DNA promoter. This may indicate that the interaction of the σ^{70} subunit with P11.60 is not specific, or that the protein possesses an RNA-specific site which may recognize similar structural features found in both the PLMVd-derived RNA template and tRNA. More importantly, it appears that despite its weakness, the binding of PLMVd-derived RNA templates to the enzyme is similar to that of a DNA promoter. This conclusion receives additional support from the demonstration that it is possible to UV-cross-link the RNAP to either the P11.60 template or the typical DNA promoter, but not to the tRNA (data not shown).

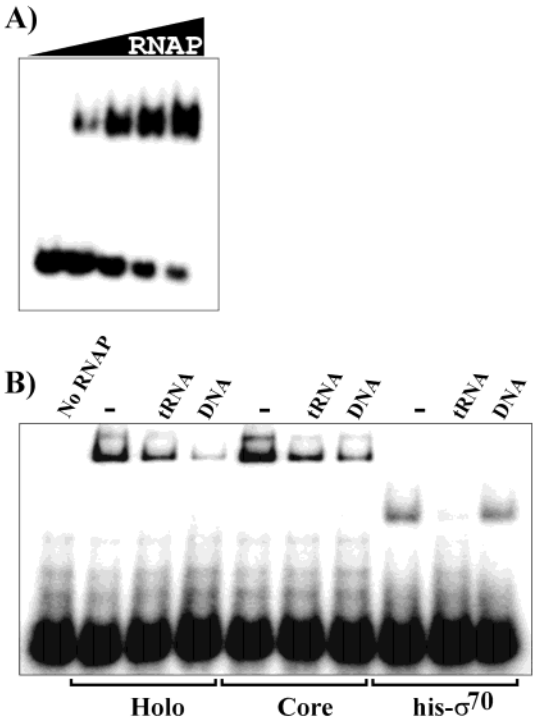

FIGURE 6: Binding affinity of PLMVd-derived RNA template with RNAP. (A) Example of an EMSA using P11.60 with increasing amounts of holo-RNAP. (B) Competition assays of P11.60 bound to holo-, core-enzyme, or his-tagged σ^{70} with either a DNA promoter or total tRNA.

DISCUSSION

E. coli RNAP Transcribes PLMVd-Derived Templates. We report here the first characterization of an RNA promoter for the *E. coli* DNA-dependent RNAP under specific conditions in vitro. Reminiscent of this RNAP acting on a canonical DNA promoter (*26*), in vitro transcription from the PLMVd-derived RNA domain incorporates an adenosine triphosphate as the initiating nucleotide. The RNA features that trigger the RNAP to initiate specific transcription are located within the left-terminal P11 domain of PLMVd. The specific structure, rather than the primary sequence of the RNA template, is important for in vitro transcription by *E. coli* RNAP. The essential requirement for this region to act

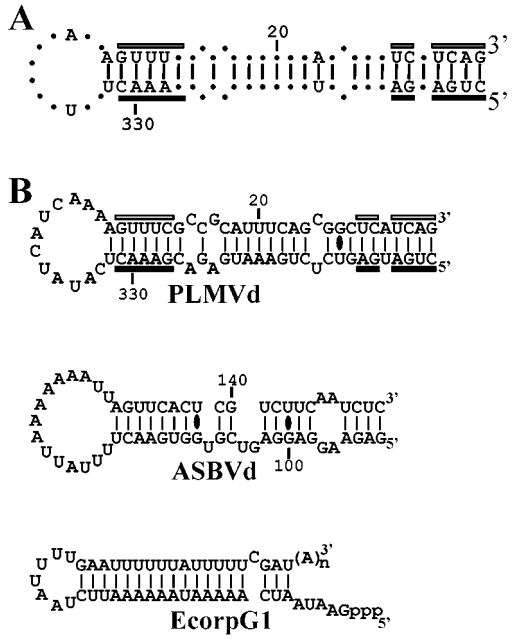

FIGURE 7: Conserved nucleotides in all natural PLMVd sequence variants and similarities to known replication systems. (A) The nucleotides conserved among the 186 sequences of the P11 domain reported to date from both polarities of the 93 PLMVd sequences naturally infecting peach plants. The strictly conserved nucleotide are shown. A dot indicates a nonconserved nucleotide. The hammerhead consensus sequences are indicated by open bars for those of minus polarity and by closed bars for those of plus polarity. Note that, with the exception of two sequences that do not harbor the guanosine from the GAAAC motif, all essential hammerhead nucleotides are conserved. (B) Sequences and secondary structures of the plus polarity strands of both the PLMVd and the ASBVd initiation regions (18, 34) and of the EcorpG1 RNA motif, which has been selected for self-propagation by *E. coli* RNAP (5).

as a promoter is that the P11 domain of PLMVd must fold into an unbranched hairpin structure possessing a basepaired uridine (U_{332}) as the first 5′-nucleotide adjacent to the loop. Any structural alterations that disrupt the overall rodlike conformation of the RNA template interfere with de novo transcription. A loop composed of at least 6 nt, and the presence of a relatively unstable stem (i.e., low GC basepairing) proximal to the loop harboring U_{332}, significantly increase the level of transcription. Most likely this locally low GC content proximal to the loop facilitates the melting of the transcriptional fork and thereby reduces the requirement for σ^{70} based melting. Recently, it was reported that the −10 region of DNA promoters exhibits a significant sequence nonspecific contribution in stabilizing *E. coli* RNAP binding when single-stranded (*29*). Perhaps the need for a single-stranded loop in the small PLMVd-derived RNA promoters reflects a comparable mechanism. A similar requirement (i.e., a single-stranded region of 6−9 nt) has been observed for other viral RNA-dependent RNAP, including those of hepatitis C virus and bovine viral diarrhea virus (*30*−*32*).

Natural variants of PLMVd possess a loop of 12 ± 1 nt at the end of the P11 stem, which may reflect differences in template requirement between in vitro transcription by the *E. coli* RNAP and the natural peach RNAP. However, in the context of an in vitro PLMVd replication system by *E. coli* RNAP, promoter efficiency may not be the best alternative for this region as it must ensure that all of the essential features of both hammerhead-mediated self-cleavage and nonenzymatic self-ligation proceed efficiently (see below). In this context, the mutations present in P11.75GC and P11.60OP could be damaging as they are located in the two most conserved regions of the hammerhead self-cleaving motif. Similarly, the reported optimal size of the loop (6−9 nt) for in vitro transcription does not take in account the need for the formation of the hammerhead secondary structure. In a PLMVd template possessing such a small loop, the formation of the hammerhead stem III could be greatly impaired (see Figure 1). A larger loop, like the one present in natural PLMVd variants, may also be justified by the existence of other selective pressures, such as the need for long-range *cis*-interactions.

E. coli RNAP requires the σ^{70} subunit to initiate in vitro transcription from PLMVd-derived RNA templates. The contribution of the σ^{70} subunit appears to be limited to its binding with core RNAP, in contrast to what is known to occur with DNA promoters where it also acts in both the fork opening and in the correct positioning of the initiation site via duplex DNA binding (*26*). However, these observations do not exclude the possibility that the σ^{70} subunit may also serve additional roles, such as supporting a conformational transition of the ternary complex or recruiting RNA templates using a putative RNA binding site.

P11 as the in Vitro Replication Domain of PLMVd. PLMVd replicates via a symmetric rolling circle mechanism involving exclusively RNA intermediates (*16*). According to this mechanism, the circular plus strand of PLMVd serves as the template for the synthesis of a multimeric minus strand which then undergoes hammerhead-mediated self-cleavage (*21*), and, most likely, a self-ligation reaction producing the circular monomeric minus strands (*33*). Using these latter species, the same three steps are repeated to generate the plus progeny. Therefore, the only step that remains unknown from this mechanism is the polymerization.

Transcription from such a PLMVd-derived template by the DNA-dependent RNAP from *E. coli* is obviously a nonphysiological reaction. However, it shares surprising similarities with the natural process implicated in the replication of PLMVd. First, the in vitro initiation sites correspond to the 5′-ends of two small PLMVd-related RNAs found in infected peach leaves. Second, the prediction of the secondary structure and analysis of base pair covariation have shown that the rodlike shape of the P11 domain is conserved among all natural PLMVd variants (*15*). This rodlike conformation was confirmed in vitro by nuclease mapping experiments coupled with binding shift assays using oligonucleotides (*14*). Third, the sequences of the P11 domains of both polarities (i.e., those corresponding to the P11.75 template) from the 93 PLMVd natural variants isolated from peach leaves, a catalog representing 186 sequences, were aligned and the perfectly conserved nucleotides were identified (Figure 7A). With the exception of two sequences that do not harbor the guanosine from the GAAAC motif, all essential hammerhead nucleotides are conserved. In addition, six residues were perfectly conserved in all known sequences: (i) the U_{316} and A_{23} that basepair and to which no function has yet been attributed; (ii) the U_{335} and A_4 that are single-stranded and have been identified as the initiation site of transcription; and; (iii) the U_{332} and A_7 that basepair and that were shown to be crucial for transcription.

These striking similarities do not completely rule out the possibility that the RNAP encoded in peach leaves behaves differently, or that long-range *cis*- and/or *trans*-acting elements are implicated in natural PLMVd replication, but they strongly suggest that a similar mechanism exists. More importantly, in vitro, the role of the P11 domain is not restricted to that of the hammerhead self-cleavage of the multimeric strands into monomers. This domain also includes all of the features required to both trigger *E. coli* RNAP and to initiate the synthesis of the complementary RNA strands, although this activity requires folding into a different secondary structure. The low GC content of the entire P11 domain may account for this structural duality. In addition, this new purpose might explain the conservation of the self-complementary character of the self-catalytic hammerhead motifs of both polarities that is responsible for generating a rodlike region.

Replication of RNA Species. The search for a similar promoter, that is a hairpin structure harboring the identified requirements, at another position within PLMVd has been fruitless, supporting the notion of an unique promoter for each strand as observed previously in the in vitro transcription from complete PLMVd RNA strands. The RNA promoter elements responsible for the initiation of transcription by *E. coli* RNAP are not unique to PLMVd, they are also found in the RNA sequences selected for self-propagation with *E. coli* RNAP (EcorpG1; Figure 7B) (*5*) and may represent something of a "universal" RNA promoter for this enzyme. These requirements for transcription from an RNA template by an RNAP also share structural similarities with those found in other natural, small, RNA pathogens. For example, replication initiation sites from ASBVd strands of both polarities share notable similarities with those found in vitro for the P11 promoter of PLMVd (i.e., the transcription starts within two large terminal loops that are next to an AU basepair and a stem with a low GC content; Figure 7B) (*34*). Also it has been observed that wheat germ DNA-dependent RNAP II could bind the large terminal loops of PSTVd (*35*). However, transcription of PSTVd by a potato RNAP II starts predominantly at two specific sites located near the central domain of the most stable rodlike structure adopted by PSTVd (*11*). Thermodynamically metastable structures, which localized the initiation sites within small hairpin domains, were proposed to be critical for PSTVd replication. Moreover, it has been reported that the replication sites and one or both of the mRNA promoters of the human hepatitis delta virus (HDV) RNA, a viroid-like RNA species, are located in close proximity to terminal hairpin loops (*36*−*41*). As is the case for in vitro transcribed PLMVd, it was reported that HDV replication depends on the secondary structure and not on the primary sequence of the RNA template (*38*). However, in this particular case, there is no initiation of replication, but instead there is utilization of the 3′-end of a cleaved HDV RNA template as primer for the initiation of HDV replication (i.e., an extension).

Obviously the in vivo characterization of the PLMVd promoter, more specifically the P11 domain, will have to be made. On the other hand, the multiple functions proposed for the domain composed solely by the hammerhead sequences render complicated the execution of such an experiment as any modification of the template may alter the levels of various activities (e.g., the self-cleavage and promoter activities). However, it seems clear that a defined hairpin-loop domain appears to be a common feature of promoters for the replication and transcription of both small natural and in vitro evolved RNA species by DNA-dependent RNAPs. Perhaps this represents an universal RNA promoter for all those RNAP. The fact that *E. coli* RNAP specifically amplifies RNA in a mechanism analogous to RNA replicase suggests that this enzyme may share several structural and mechanistic features with RNA-dependent RNAPs.

ACKNOWLEDGMENT

We thank J. Gralla for providing *rpo*D wild-type and mutant harboring plasmids.

REFERENCES

1. Konarska, M. M., and Sharp, P. A. (1989) Replication of RNA by the DNA-dependent RNA polymerase of phage T7. *Cell 57*, 423−431.
2. Biebricher, C. K., and Luce, R. (1996) Template-free generation of RNA species that replicate with bacteriophage T7 RNA polymerase. *EMBO J. 15*, 3458−3465.
3. Rohde, W., Rackwitz, H. R., Boege, F., and Sanger, H. L. (1982) Viroid RNA is accepted as a template for in vitro transcription by DNA-dependent DNA polymerase I and RNA polymerase from *Escherichia coli*. *Biosci. Rep. 2*, 929−939.
4. Biebricher, C. K., and Orgel, L. E. (1973) An RNA that multiplies indefinitely with DNA-dependent RNA polymerase: selection from a random copolymer. *Proc. Natl. Acad. Sci. U.S.A. 70*, 934−938.
5. Wettich, A., and Biebricher, C. K. (2001) RNA species that replicate with DNA-dependent RNA polymerase from *Escherichia coli*. *Biochemistry 40*, 3308−3315.
6. Flores, R., Daros, J. A., and Hernandez, C. (2000) Avsunviroidae family: viroids containing hammerhead ribozymes. *Adv. Virus Res. 55*, 271−323.
7. Schindler, I. M., and Muhlbach, H. P. (1992) Involvement of nuclear DNA-dependent RNA polymerases in potato spindle tuber viroid replication: a reevaluation. *Plant Sci. 84*, 221−229.
8. Bonfiglioli, R. G., Webb, D. R., and Symons, R. H. (1996) Tissue and intracellular distribution of coconut cadang cadang viroid and citrus exocortis viroid determined by in situ hybridization and confocal laser scanning and transmission electron microscopy. *Plant J. 9*, 457−465.
9. Harders, J., Lukacs, N., Robert-Nicoud, M., Jovin, J. M., and Riesner, D. (1989) Imaging of viroids in nuclei from tomato leaf tissue by in situ hybridization and confocal laser scanning microscopy. *EMBO J. 8*, 3941−3949.
10. Warrilow, D., and Symons, R. H. (1999) Citrus exocortis viroid RNA is associated with the largest subunit of RNA polymerase II in tomato *in vivo*. *Arch. Virol. 144*, 2367−75.
11. Fels, A., Hu, K., and Riesner, D. (2001) Transcription of potato spindle tuber viroid by RNA polymerase II starts predominantly at two specific sites. *Nucleic Acids Res. 29*, 4589−4597.
12. Flores, R., Navarro, J. A., de la Pena, M., Navarro, B., Ambros, S., and Vera, A. (1999) Viroids with hammerhead ribozymes: some unique structural and functional aspects with respect to other members of the group. *Biol. Chem. 380*, 849−854.
13. Navarro, B., and Flores, R. (1997) Chrysanthemum chlorotic mottle viroid: unusual structural properties of a subgroup of self-cleaving viroids with hammerhead ribozymes. *Proc. Natl. Acad. Sci. U.S.A. 94*, 11262−11267.
14. Bussière, F., Ouellet, J., Côté, F., Lévesque, D., and Perreault, J. P. (2000) Mapping in solution shows the peach latent mosaic viroid to possess a new pseudoknot in a complex, branched secondary structure. *J. Virol. 74*, 2647−2654.
15. Pelchat, M., Lévesque, D., Ouellet, J., Laurendeau, S., Lévesque, S., Lehoux, J., Thompson, D. A., Eastwell, K. C., Skrzeczkowski, L. J., and Perreault, J. P. (2000) Sequencing

of peach latent mosaic viroid variants from nine North American peach cultivars shows that this RNA folds into a complex secondary structure. *Virology 271*, 37−45.
16. Bussière, F., Lehoux, J., Thompson, D. A., Skrzeczkowski, L. J., and Perreault, J. P. (1999) Subcellular localization and rolling circle replication of peach latent mosaic viroid: hallmarks of group A viroids. *J. Virol. 73*, 6353−6360.
17. Navarro, J. A., Daros, J. A., and Flores, R. (1999) Complexes containing both polarity strands of avocado sunblotch viroid: identification in chloroplasts and characterization. *Virology 253*, 77−85.
18. Stern, D. B., Higgs, D. C., and Yang, J. (1997) Transcription and translation in chloroplasts. *Trends Plant Sci. 2*, 308−315.
19. Navarro, J. A., Vera, A., and Flores, R. (2000) A chloroplastic RNA polymerase resistant to tagetitoxin is involved in replication of avocado sunblotch viroid. *Virology 268*, 218−225.
20. Pelchat, M., Côté, F., and Perreault, J. P. (2001) Study of the polymerization step of the rolling circle replication of peach latent mosaic viroid. *Arch. Virol. 146*, 1753−1763.
21. Beaudry, D., Bussière, F., Lareau, F., Lessard, C., and Perreault, J. P. (1995) The RNA of both polarities of the peach latent mosaic viroid self-cleaves in vitro solely by single hammerhead structures. *Nucleic Acids Res. 23*, 745−752.
22. Fenton, M. S., Lee, S. J., and Gralla, J. D. (2000) *Escherichia coli* promoter opening and −10 recognition: mutational analysis of sigma70. *EMBO J. 19*, 1130−1137.
23. Wilson, C., and Dombroski, A. J. (1997) Region 1 of sigma70 is required for efficient isomerization and initiation of transcription by *Escherichia coli* RNA polymerase. *J. Mol. Biol. 267*, 60−74.
24. Gagnon, Y., Breton, R., Putzer, H., Pelchat, M., Grunberg-Manago, M., and Lapointe, J. (1994) Clustering and co-transcription of the *Bacillus subtilis* genes encoding the aminoacyl-tRNA synthetases specific for glutamate and for cysteine and the first enzyme for cysteine biosynthesis. *J. Biol. Chem. 269*, 7473−7482.
25. Hawley, D. K., and McClure, W. R. (1983) Compilation and analysis of *Escherichia coli* promoter DNA sequences. *Nucleic Acids Res. 11*, 2237−2255.
26. Record, M. T. J., Reznikoff, W. S., Craig, M. L., McQuade, K. L., and Schlax, P. J. (1996) in *Escherichia coli and Salmonella: Cellular and Molecular Biology* (Neidhardt, F. C. Ed.) pp 792−820, Am. Soc. Microbiol., Washington, DC.
27. Zuker, M., Mathews, D. H., and Turner, D. H. (1999) Algorithms and Thermodynamics for RNA Secondary Structure Prediction: A Practical Guide, in *RNA Biochemistry and Biotechnology* (Barciszewski, J., and Clark, B. F. C. Eds.) pp 11−43, NATO ASI Series, Kluwer Academic Publishers.
28. Helmann, J. D., and deHaseth, P. L. (1999) Protein-nucleic acid interactions during open complex formation investigated by systematic alteration of the protein and DNA binding partners. *Biochemistry 38*, 5959−5967.
29. Fenton, M. S., and Gralla, J. D. (2001) Function of the bacterial TATAAT −10 element as single-stranded DNA during RNA polymerase isomerization. *Proc. Natl. Acad. Sci. U.S.A. 98*, 9020−9025.
30. Sun, X. L., Johnson, R. B., Hockman, M. A., and Wang, Q. M. (2000) *De novo* RNA synthesis catalyzed by HCV RNA-dependent RNA polymerase. *Biochem. Biophys. Res. Commun. 268*, 798−803.
31. Zhong, W., Ferrari, E., Lesburg, C. A., Maag, D., Ghosh, S. K., Cameron, C. E., Lau, J. Y., and Hong, Z. (2000) Template/primer requirements and single nucleotide incorporation by hepatitis C virus nonstructural protein 5B polymerase. *J. Virol. 74*, 9134−9143.
32. Kim, M. J., Zhong, W., Hong, Z., and Kao, C. C. (2000) Template nucleotide moieties required for *de novo* initiation of RNA synthesis by a recombinant viral RNA-dependent RNA polymerase. *J. Virol. 74*, 10312−10322.
33. Côté, F., Lévesque, D., and Perreault, J. P. (2001) Natural 2′,5′-phosphodiester bonds found at the ligation sites of peach latent mosaic viroid. *J. Virol. 75*, 19−25.
34. Navarro, J. A., and Flores, R. (2000) Characterization of the initiation sites of both polarity strands of a viroid RNA reveals a motif conserved in sequence and structure. *EMBO J. 19*, 2662−2670.
35. Goodman, T. C., Nagel, L., Rappold, W., Klotz, G., and Riesner, D. (1984) Viroid replication: equilibrium association constant and comparative activity measurements for the viroid-polymerase interaction. *Nucleic Acids Res. 12*, 6231−6246.
36. Beard, M. R., MacNaughton, T. B., and Gowans, E. J. (1996) Identification and characterization of a hepatitis *delta* virus RNA transcriptional promoter. *J. Virol. 70*, 4986−4995.
37. Modahl, L. E., and Lai, M. M. C. (1998) Transcription of hepatitis *delta* antigen mRNA continues throughout hepatitis *delta* virus (HDV) replication: a new model of HDV RNA transcription and replication. *J. Virol. 72*, 5449−5456.
38. Filipovska, J., and Konarska, M. M. (2000) Specific HDV RNA-templated transcription by pol II in vitro. *RNA 6*, 41−54.
39. Gudima, S., Wu, S.-Y., Chiang, C.-M., Moraleda, G., and Taylor, J. (2000) Origin of hepatitis *delta* virus mRNA. *J. Virol. 74*, 7204−7210.
40. Chang, J., Sigal, L. J., Lerro, A., and Taylor, J. (2001) Replication of the human hepatitis *delta* virus genome is initiated in mouse hepatocytes following intravenous injection of naked DNA or RNA sequences. *J. Virol. 75*, 3469−3473.
41. Gudima, S., Dingle, K., Wu, T. T., Moraleda, G., and Taylor, J. (1999) Characterization of the 5′ ends for polyadenylated RNAs synthesized during the replication of hepatitis *delta* virus. *J. Virol. 73*, 6533−6539.

BI025595K